ADVANCED MATERIALS
www.advmat.de

In Situ Architectures Designed in 3D Cell-Laden Hydrogels Using Microscopic Laser Photolithography

*Iris Mironi-Harpaz, Lena Hazanov, Guy Engel, Dvir Yelin, and Dror Seliktar**

The ability to apply photochemistry and microscopic patterning techniques for making hydrogel scaffolds enables formation of heterogeneous mechanical structures and chemical gradients that can guide tissue morphogenesis and control stem cell fate.[1] Microscopy-guided methods to pattern cell-laden hydrogels with micrometer-scale 3D features have been hampered by the complexity of the localized photochemical interactions. This is because cell-compatible hydrogels contain dilute solutions and limited amounts of photoinitiator – resulting in crosslinking reactions on timescales of seconds to minutes.[2,3] In addition, the distances traversed by the macromolecular polymer chains in the solution during the time scale that would be required for photochemical network formation are much larger compared to the spot size of the laser beam used for photoinitiation.[4] In effect, the polymers constantly entering and exiting the illuminated volume cannot properly conjugate, resulting in localized free-radical polymerization that is inherently unable to form a contiguous hydrogel network in the illuminated spot, irrespective of the illumination time.

This limitation could be overcome without additional chemistries, either by slowing down the transport kinetics of the macromolecular polymer chains or by increasing the concentration of functional groups and reactive radicals in the precursor solution for speeding up the polymerization process. In the case of the latter, however, a highly crosslinked polymer network is formed that is incompatible with most in situ 3D cell cultivation.[5] Alternatively, cytotoxic levels of radicals can be detrimental to the cells in the chemically crosslinked photopatterned regions.[6] Hence, alterations to transport kinetics have been used more successfully to pattern hydrogels that are more compatible with in situ 3D cell culture. The hydrogels are usually irreversibly and chemically crosslinked to immobilize the polymer chains,[7–9] followed by additional photoinitiated free-radical crosslinking localized to the regions of illumination.[10] Nevertheless, some of these techniques still fall short of providing a hospitable environment for 3D cell culture during and after microscopic photopolymerization is achieved.[11,12] Here, we tested a method to micropattern hydrogels using a reversible temperature-induced phase transition from liquid to solid vis-à-vis lower critical solubility temperature (LCST) in order to facilitate reduced transport kinetics of the polymer chains in solution, thus enabling mild microscopic photochemical crosslinking that is compatible with cell-laden 3D culture. The confluence of a thermal gelation in tandem with a chemical crosslinking by photopolymerization culminates in an irreversibly crosslinked contiguous polymer network at the focal region of the microscope objective lens. The result is a cell-laden hydrogel with dispersed cells cultivated in 3D within a material having small-scale architectures that guide cellular morphogenesis based on material interactions.

Cell-compatible LCST hydrogel materials were synthesized using semisynthetic adducts of fibrinogen and functionalized poloxamer (ethylene oxide/propylene oxide block copolymer) (**Figure 1**). The fibrinogen provides the basic bioactive features essential for in situ 3D cell culture, including adhesion and proteolytic susceptibility.[13] The functionalized poloxamers provide the reactive groups that are responsible for the mild photochemistry leading to covalent bond formation, as well as for the LCST properties.[14] The poloxamer Pluronic F127 was chosen because it was able to facilitate a phase transition below 37 °C; the concentrations of constituents and photoinitiator were chosen to allow in situ 3D cell culture with low cytotoxicity (>85% cell viability after 3 days in culture).[15] Physical crosslinking of the Pluronic F127-fibrinogen adducts (Pluronic–fibrinogen) occurs upon temperature elevation from 20 to 37 °C (Figure 1 and the Supporting Information).

Patterned photochemistry of the Pluronic–fibrinogen hydrogels was performed using an inverted microscope setup with a temperature-controlled stage (**Figure 2**a). Illumination from a nanosecond pulse UV (355 nm) laser was used for initiating the free-radical polymerization of the Pluronic–fibrinogen containing photoinitiator (Irgacure 2959, CIBA). With the stage-incubator set to a temperature of 37 °C, the positioning of the focal region within the Pluronic–fibrinogen construct enabled pinpoint covalent crosslinking with spatial resolutions that depend mainly on the illuminating beam waist. A variable aperture at the back focal plane of the objective lens was used to control the beam diameter, while widefield transmission microscopy using visible light was used to monitor the patterning process. In order to verify covalent reaction, rhodamine-labeled Pluronic F127-acrylate (red) was added to the Pluronic–fibrinogen and co-immobilized in regions of chemical crosslinking (Figure 2b). Poly(ethylene glycol) (PEG)-coated fluorescein isothiocyanate (FITC) polystyrene microbeads embedded in the Pluronic–fibrinogen constructs were used to map spatial variations in material properties associated with physical/chemical (Figure 2b, inner) versus physical (Figure 2b, outer) crosslinked regions. Comparing the mean square displacements (MSD) of the beads within chemically physically crosslinked regions to those of beads located in physically crosslinked regions (Figure 2c), we confirmed a statistically significant increase in the storage component of the complex shear modulus (n = 20,

Dr. I. Mironi-Harpaz, L. Hazanov, G. Engel,
Prof. D. Yelin, Prof. D. Seliktar
Faculty of Biomedical Engineering
Technion – Israel Institute of Technology
Haifa 32000, Israel
E-mail: dror@bm.technion.ac.il

DOI: 10.1002/adma.201404185

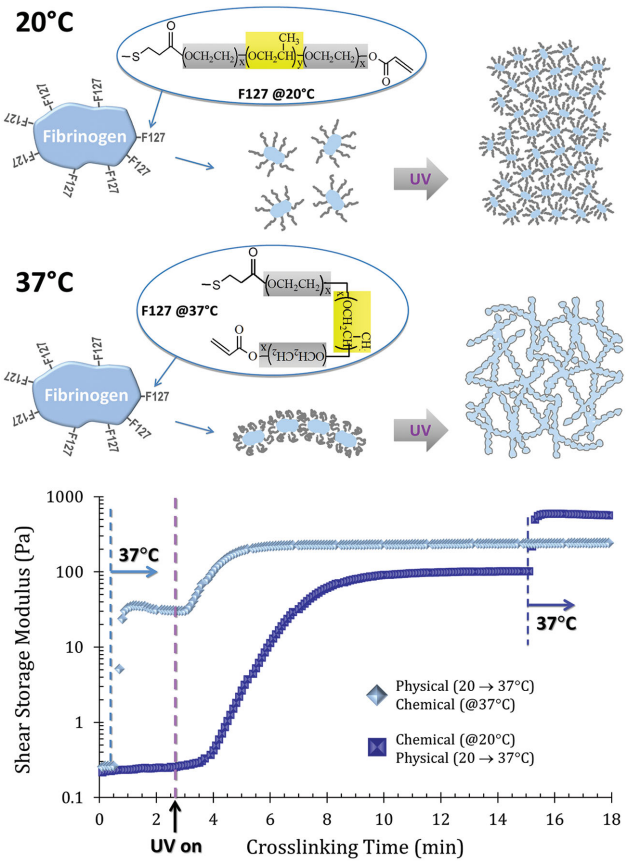

Figure 1. Bioactive hydrogels made to exhibit LCST are obtained by conjugating fibrinogen with functionalized Pluronic F127. A base/nucleophile-initiated thiol-ene reaction results in Fibrinogen-F127 adducts (Pluronic–fibrinogen) containing pendent reactive acrylate end-groups. The Pluronic–fibrinogen is physically crosslinked by increasing ambient temperature to 37 °C, and/or chemically crosslinked by UV light-activated photochemistry. Graph: Formation of an elastic hydrogel network and its bulk mechanical properties are measured using a stress controlled shear rheometer with temperature stabilization and a UV curing attachment. The storage component of the complex shear modulus demonstrates the LCST behavior coupled with photochemical crosslinking of the Pluronic–fibrinogen adducts.

$p < 0.01$) (Figure 2d). Similar results were obtained when comparing bulk Pluronic–fibrinogen hydrogels uniformly physically crosslinked (by temperature alone at 37 °C) to hydrogels that were uniformly chemically/physically crosslinked (by UV illumination at 37 °C) ($n = 20$, $p < 0.01$). Changes in the shear storage modulus values measured by microrheology (Figure 2d) were in agreement with the changes observed by parallel plate shear rheology (Figure 1).

Chemically crosslinking the Pluronic–fibrinogen hydrogels in small confined volumes was achieved by illumination with a narrow UV laser beam while the high-viscosity physical gel restricted mobility of the Pluronic–fibrinogen macromolecules in and around the illuminated region. In dilute low-viscosity solutions of macromolecular polymer chains, the free-radical formation of chemical bonds can take at least several seconds,[16] with illumination power and spot volume also affecting the reaction kinetics.[4] In contrast, macromolecular diffusion in the physical hydrogel precursor solution was far slower, providing sufficient time to facilitate transport of functional groups and radicals towards the critical proximity required for a reaction to culminate in crosslinks. Because the photochemical process is nearly linearly proportional to the laser intensity, arbitrary 3D structures were difficult to produce using tightly focused beams. 3D patterning could be achieved by varying the beam diameter within the sample, for example, by using converging beams for creating conical formations or by using more sophisticated holographic masks for forming arbitrary 3D patterns. At spatial resolutions below several tens of micrometers, however, diffusion of reactive radicals from the illuminated volume would become dominant, preventing patterning resolutions to drop into the micrometer scale.

In a set of control patterning experiments, the Pluronic–fibrinogen was illuminated using the inverted microscope setup with the stage-incubator set to a temperature of 15 °C (below the critical gelation temperature of the hydrogel precursor). Rhodamine-labeled Pluronic F127-acrylate (red) was added to the Pluronic–fibrinogen to verify any chemical crosslinking. There was no evidence of chemically crosslinked patterns when the hydrogel precursor temperature was set at 15 °C (the Supporting Information). In contrast, patterns were evident when the hydrogel precursor temperature was set to 25 or 37 °C. In another set of control experiments performed identically using hydrogel precursors based on PEG–fibrinogen polymers that lack LCST properties, we were unable to yield a contiguous polymer network in the microscopic spot of the system when the hydrogel precursor temperature was set at 37 °C (the Supporting Information). The PEG–fibrinogen adducts are almost identical to the Pluronic F127-fibrinogen adducts in terms of molecular weight and polymer chain length. Hence, the photopatterning system required the LCST properties when crosslinking the reactive macromolecular hydrogel precursors in dilute solutions. Several shapes and patterns were produced by illuminating the 37 °C temperature-stabilized physical hydrogels by a 135-μm-diameter UV (355 nm) pulse (1 ns, 100 Hz repetition rate) laser beam at 3 pJ per pulse (**Figure 3**). Effective crosslinking was achieved by scanning the laser beam over the sample at a constant speed of 1 mm s^{-1} a minimum of four repeats (1 Hz repetition rate), corresponding to a total fluence of 1.13 μJ cm^{-2} for each illuminated region. Exposing the material to less UV illumination did not culminate in consistent chemical crosslinking and resulted in patterns with lower fidelity. Exposing the material to more UV illumination affected the size of the columns, presumably due to the diffusion of free radicals from the illumination volume and/or effects associated with the propagation phase of the free-radical polymerization reaction.

Human dermal fibroblast cells (hDFs) expressing green fluorescent protein (GFP) were suspended in Pluronic–fibrinogen solution at 20 °C, then cast into microscope slide chambers and physically crosslinked by incubation at 37 °C. Using the microscope-guided laser patterning system, columnar patterns (**Figure 4**a) were then produced in the cell-laden physical Pluronic–fibrinogen hydrogels using different illumination times (i.e., multiple scans of the material). The columns of 170-μm-diameter cylindrical regions ($G' \approx 200$ Pa, chemical–physical crosslinking) within the softer hydrogel ($G' \approx 35$ Pa,

Adv. Mater. **2015**,
DOI: 10.1002/adma.201404185

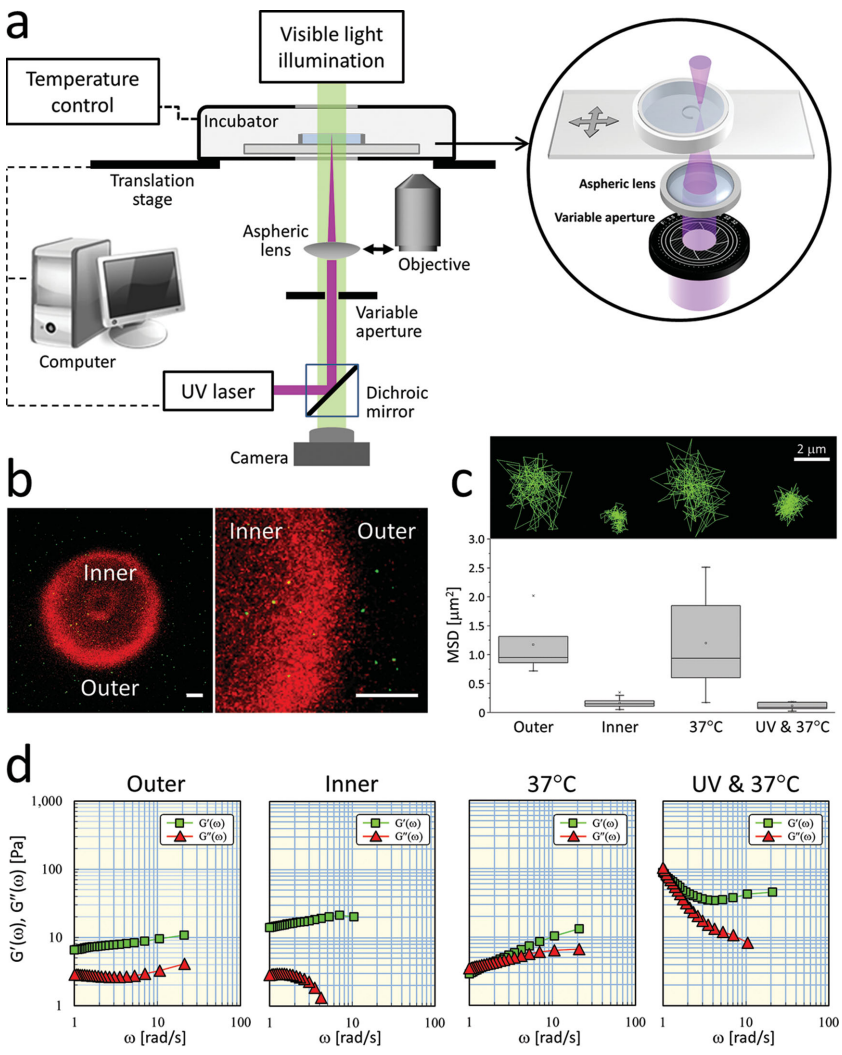

Figure 2. The experimental setup for laser-based chemical crosslinking of Pluronic–fibrinogen hydrogels shows the various components of the optical system (a), including the beam focusing optics shown in a close-up view. Microrheology used to ascertain the localized mechanical effects of chemical and/or physical crosslinking of Pluronic–fibrinogen employ polystyrene microbeads (green dots, 0.2 μm diameter) embedded in the hydrogels (b). Microbeads within the photopatterned region (red) of the gel exhibit MSD values that are significantly lower than elsewhere in the gel ($n = 20$, $p < 0.01$) (c). The corresponding storage shear modulus values in these regions are significantly higher ($n = 20$, $p < 0.01$) – consistent with the microrheology properties measured for bulk hydrogels made under similar crosslinking conditions (d). Scale bars = 100 μm.

physical crosslinking only) were created in the presence of cells by four repeated scans of the 135-μm-diameter beam with a total fluence of 1.13 μJ cm^{-2} (Figure 4b). Different UV exposures of the spot increased the size of columns (Figure 4a), but did not seem to affect the behavior of the cells. We note here that Shachaf et al. evaluated cell viability in Pluronic F127-fibrinogen hydrogels uniformly crosslinked with UV light (365 nm) at 37 °C, with a total fluence of orders of magnitude higher (1.2 J cm^{-2}); they found cell viability was >88% after 1 day and >85% after 3 days.[15]

Initially, cells responded to the stiffer regions by remaining less spindled as compared to the higher spindled morphology of the cells in the softer regions (Figure 4b and the Supporting Information). Immobilized Rhodamine-labeled Pluronic F127-acrylate confirmed a chemical crosslinking reaction and verified that cells responded to the stiffer regions by encircling the columns, eventually forming a thick multicellular cylindrical network that constricts the stiffer core (Figure 4a,c). Cells responded differently when the stiffer columnar patterns were made with a softer center region (Figure 4d); highly spindled cells were observed in the soft regions and stiffer regions inhibited spindled cell morphogenesis, but no constriction was evident. The degree of crosslinking in a hydrogel matrix may also affect its susceptibility to proteolysis as more crosslinks must be degraded to dissociate the polymer network. We previously characterized the rate of proteolysis of Pluronic F127-fibrinogen hydrogels and found that the additional chemical crosslinking mildly affected the susceptibility of the fibrinogen backbone to protease degradation.[15] Thus we cannot rule out the possibility that the cells were also responding to the changing degradability of the stiff regions.

Cultivating the hDFs in control hydrogels that were uniformly crosslinked (Figure 4b) showed a similar morphogenesis pattern associated with each respective homogenous material (the Supporting Information), further supporting the potential role of interfacial properties of structural landscapes in 3D tissue morphogenesis. Notably, the minor alterations in shear storage modulus within the matrix – approximately 165 Pa difference between the stiff and soft regions – caused prominent morphological patterns in the cell-laden hydrogels at the interface between the regions.

In summary, we demonstrated that 3D stiffness landscaping of hydrogels based on tandem physical and chemical photolithographic crosslinking at high spatial resolutions can be used to fashion bioactive scaffolds with ten-micrometer-scale structural features in the presence of cells. We have also identified unique behavior of fibroblasts to interfacial patterns in 3D culture, even with the smallest of changes in physical landscape (shear storage modulus changes of <165 Pa). We believe that these results represent a significant step towards realizing the true potential of biological soft matter photolithography. Future experiments using more specialized cell types can help elucidate the precise role that minute changes in physical landscapes have on embryonic morphogenesis as well as on tissue repair processes. For example, the technique can be applied to hierarchically organize cells into tissue-like structures with spatial presentations that mediate multicellular morphogenesis. Photochemically landscaped cell-laden hydrogels can likewise be used to investigate stem cell fate by regulating the biomimetic niche, including patterns of growth

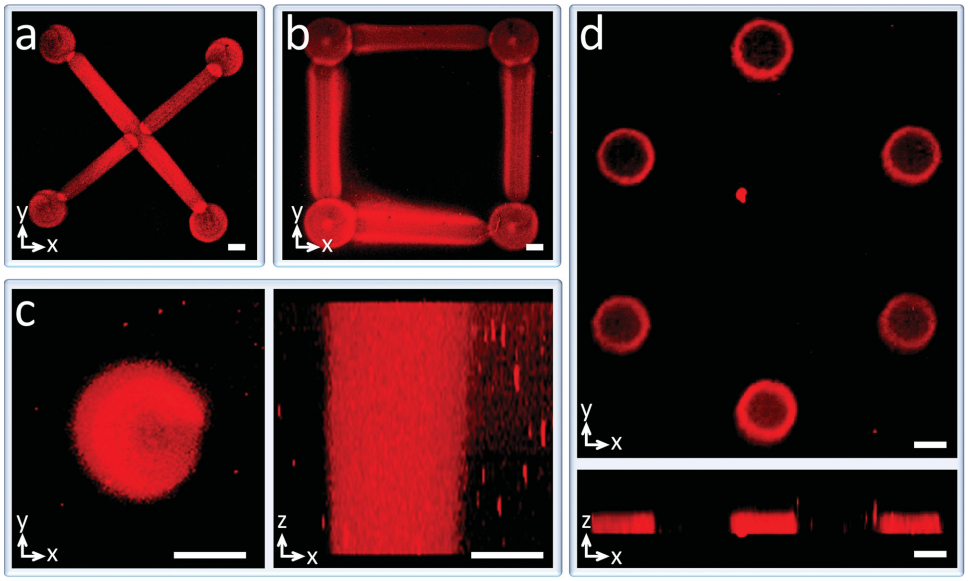

Figure 3. Photopatterning of temperature-stabilized (37 °C) physical hydrogels made from Pluronic–fibrinogen using a UV (355 nm) pulsed laser beam. The chemical crosslinking reaction was achieved by repeatedly scanning the laser beam over the sample with a total fluence of 1.13 μJ cm^{-2}. Rhodamine-labeled Pluronic F127-acrylate (red) was added to the Pluronic–fibrinogen and co-immobilized in regions of chemical crosslinking to verify a covalent reaction. Distinct 2D patterns are obtained by moving the microscope stage in two dimensions (a,b). 3D columnar structures of different heights are crosslinked as revealed by confocal microscopy top and side views of a single (c) and multiple (d) columns. Scale bars = 100 μm.

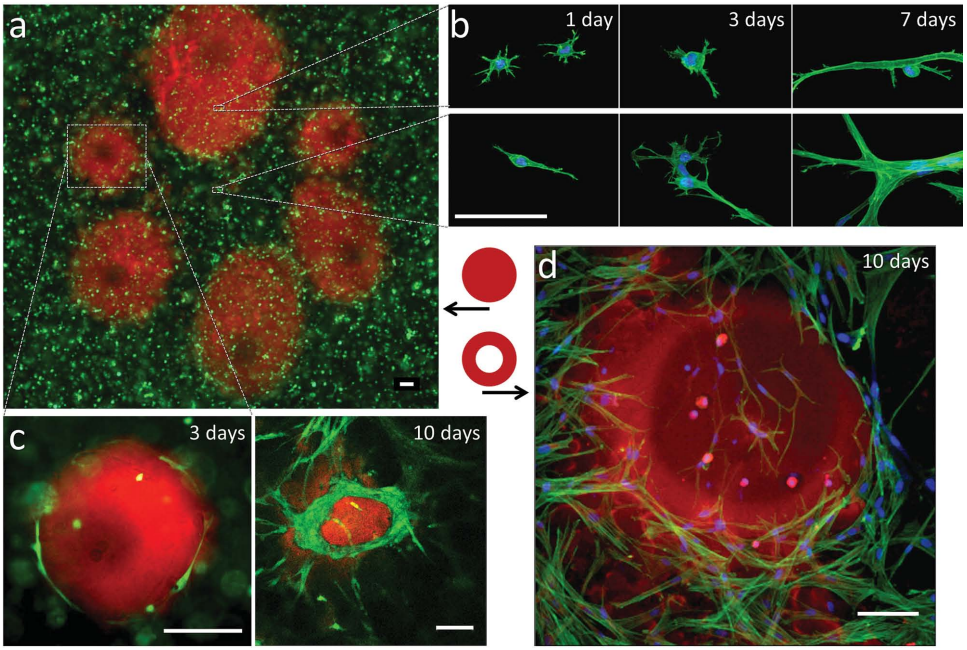

Figure 4. Photopatterning of cell-laden Pluronic–fibrinogen hydrogels influences in situ cellular morphogenesis. GFP-expressing fibroblasts are cultured within a physically crosslinked hydrogel of Pluronic–fibrinogen with rhodamine-labeled Pluronic F127-acrylate (red) co-immobilized in regions of chemical crosslinking (a). The cells (in green) orient at the interface between the stiff regions (in red) and the softer regions (in black). Different exposure times are shown in (a) to demonstrate the effects on the cell behavior and pattern size. Fibroblasts grown in control hydrogels (not patterned) with physical–chemical crosslinking (b, top) or physical crosslinking alone (b, bottom) exhibited different time-dependent morphological features, which were consistent with their respective environments in the patterned system (the Supporting Information). The mechanical landscape of the Pluronic–fibrinogen hydrogels affects the cellular morphogenesis particularly at the interface between the stiff and soft regions, as indicated after 10 days in cultures with columnar patterns that are solid (c) or hollow (d). GFP-labeled cells (green) with rhodamine-labeled Pluronic F127-acrylate (red) are shown in (a,c); FITC-phalloidin (green) with DAPI nuclear staining is shown in b) and combined with rhodamine-labeled Pluronic F127-acrylate (red) in (d). Scale bars = 100 μm.

Adv. Mater. **2015**,
DOI: 10.1002/adma.201404185

factors, cytokines, chemokines and biophysical properties. Using new patterning paradigms that can overcome the limitations of existing techniques, the field gains the ability to develop sophisticated material systems for conducting basic and applied biomedical research, developing biosensors and creating functional tissue mimics.

Experimental Section

Pluronic F127-Fibrinogen Adducts: Temperature-responsive bioactive hydrogels were made from fibrinogen conjugated to Pluronic F127 (F127), a poly(ethylene oxide) (PEO)–poly(propylene oxide)–PEO triblock copolymer that exhibits LCST properties. The F127 was end-functionalized with acryl groups to form F127-diacrylate (F127-DA) and then reacted with denatured fibrinogen via a Michael-type addition reaction to form the Pluronic–fibrinogen biosynthetic copolymer.[15] For fluorescence labeling experiments, Rhodamine B isothiocyanate (RITC)–F127-acrylate was synthesized by conjugating RITC to F127 on one of the hydroxyl groups, followed by end-functionalization of the other hydroxyl group with an acrylate group. The RITC-Pluronic F127-DA was added (0.05% w/v) to the hydrogel precursor prior to the photopatterning experiments and the unreacted RITC-Pluronic F127-DA was removed out of the hydrogel by multiple sequentially washes in phosphate buffered saline (PBS) afterwards. In order to allow chemical crosslinking within the bulk material using photolithography, the material's light scattering was reduced by adding F127-DA (1% w/v) to the Pluronic–fibrinogen.

Bulk Rheology: Mechanical properties of the Pluronic–fibrinogen were characterized with a stress-controlled shear rheometer (AR-G2, TA Instruments) equipped with a Peltier plate temperature-controlled base, an overhead UV curing assembly and transparent geometry. Time-sweep oscillatory tests were performed in the linear viscoelastic region (at 2% strain and 1 Hz frequency) using a 50 mm parallel-plate quartz geometry with 600 µL of Pluronic–fibrinogen precursor solution containing 0.3% w/v Irgacure 2959 initiator (Ciba, Basel, Switzerland) and 1% w/v F127-DA. In order to monitor the in situ liquid-to-gel transition (physical gelation), the precursor solution was first kept at 20 °C for 8 min during which after 1 min of equilibration it was exposed to UV light (365 nm, 2 mW cm^{-2}) for 12.5 min. Then, the temperature was raised to 37 °C and held for 5 min. Alternatively, after 0.5 min of equilibration at 20 °C, the precursor solution temperature was raised to 37 °C and held for 2 min. After that time, the sample was exposed to UV light until the end of the experiment. In order to find the linear viscoelastic region of the time-sweep tests, oscillatory strain (0.1–10%) and frequency sweeps (0.1–10 Hz) were conducted in two separate samples at 20 °C (following the exposure to UV light) and at 37 °C (the temperature was raised to 37 °C after exposure to UV light at 20 °C, as before).

Particle Tracking Microrheology: Polystyrene microbeads (PEG-coated, FITC-labeled, 0.2 µm diameter) were embedded in crosslinked Pluronic–fibrinogen hydrogels, equilibrated for 1 h and imaged using a ×63, NA = 0.9 water immersion objective lens. Particle motion was documented for 20 individual microbeads at 20 frames s^{-1} for 10 s (up to 33 ms exposure time). The particle position vectors and trajectories were determined using an image analysis algorithm in order to calculate their MSD.[17] The ensemble averaged MSD (2D) was used to obtain the approximate complex shear modulus using the generalized Stokes–Einstein relation based on a method proposed by Dasgupta.[18] Algorithms developed by Kilfoil were used to automate the analysis using MATLAB software.[19] Statistical analysis of the ensemble MSD curves of the different treatments was performed using the diffusion coefficient method proposed by Ernst and Kohler.[20]

Microscope System: The hydrogel samples were placed within a compact stage incubator (Zeiss, Germany) that provided dynamic control over temperature and CO_2 levels. Sample illumination by a UV laser beam was achieved using a PALM MicroBeam system (Carl Zeiss MicroImaging, Bernried, Germany) equipped with a nanosecond laser (1 ns pulses, 100 Hz frequency, 355 nm wavelength, up to 90 mJ per pulse), a computer-controlled translation stage and a custom-built low numerical aperture (NA) focusing optics comprised of an aspheric lens and a variable aperture. In the experiment, a fixed 1.35-mm-diameter aperture and a 50-mm-focal-length lens were used to illuminate (NA = 0.014) the samples, which were placed approximately 5 mm above the focal plane of the beam, resulting in an averaged 135-mm-diameter illumination spot. Scanning was performed by moving the motorized stage at a speed of 1 mm s^{-1} using the system's software that provides full control over the mechanical shutter, beam intensity and scan speed in three dimensions. Visible-light wide-field imaging was used to guide the crosslinking process in real time through the same beam-focusing optics.

Cell Seeded Pluronic–Fibrinogen Experiments: Neo-natal human dermal fibroblasts (hDFs) (Lonza (Visp, Switzerland)) expressing GFP were cultured in Dulbecco's modified Eagle's medium (Gibco, UK) containing 10% fetal bovine serum (Biological Industries, Israel), 1% penicillin–streptomycin (Biological Industries), 1% L-glutamine (Gibco), 0.2% 2-mercaptoethanol (Gibco), and 1% non-essential amino acid solution (Biological Industries). Cellularized constructs were prepared through physical crosslinking of the biopolymer precursor solution (7 mg mL^{-1} fibrinogen) with dispersed hDFs (1×10^6 cells mL^{-1}) by elevating the temperature from 20 to 37 °C. Localized photopolymerization in predefined patterns was applied on physically crosslinked samples containing 0.3% Irgacure 2959 photoinitiator in the laser microscope system. Cell morphology was documented using high-resolution laser scanning confocal microscopy. Cell-seeded hydrogel constructs (not expressing GFP) were stained with FITC–phalloidin (Sigma–Aldrich) and a 4′,6-diamidino-2-phenylindole (DAPI) nuclear counterstain (Sigma–Aldrich). Whole mounts were imaged with a Zeiss LSM700 scanning confocal microscope.

Statistical Analysis: Data were expressed as group mean ± standard deviations, unless specified otherwise. The statistical analyses were performed using Student's *t*-test or a two-way repeated-measures analysis of variance (ANOVA) test to compare multiple data groups, followed by Fisher's least significant difference (LSD) posthoc test. Significance was established at $p < 0.05$.

Supporting Information

Supporting Information is available from the Wiley Online Library or from the author.

Acknowledgements

Support was provided in part by the European Union EC-IP FP7 grants Angioscaff and Biodesign (DS, LH), the European Research Council grant 239986 (DY, IMH), the Lorry I. Lokey Interdisciplinary Center for Life Sciences and Engineering, and the Russell Berrie Nanotechnology Institute. I.M.-H. and L.H. designed and performed the experiments, analyzed data, and prepared the paper. G.E. designed and performed the lithography and mircrorheology experiments. D.Y. directed the research, designed the optical system, designed the photolithography experiments, analyzed data, and prepared the paper. D.S. directed the research, designed the experiments, analyzed data, and prepared the paper.

Received: September 10, 2014
Revised: January 8, 2015
Published online:

[1] S. Khetan, J. A. Burdick, *Soft Matter* **2011**, *7*, 830.
[2] I. Mironi-Harpaz, D. Y. Wang, S. Venkatraman, D. Seliktar, *Acta Biomater.* **2012**, *8*, 1838.
[3] M. P. Schwartz, B. D. Fairbanks, R. E. Rogers, R. Rangarajan, M. H. Zaman, K. S. Anseth, *Integr. Biol.* **2010**, *2*, 32.
[4] T. F. Scott, B. A. Kowalski, A. C. Sullivan, C. N. Bowman, R. R. McLeod, *Science* **2009**, *324*, 913.

[5] S. Kawata, H. B. Sun, T. Tanaka, K. Takada, *Nature (London)* **2001**, *412*, 697.
[6] A. Ovsianikov, S. Muhleder, J. Torgersen, Z. Li, X. H. Qin, S. Van Vlierberghe, P. Dubruel, W. Holnthoner, H. Redl, R. Liska, J. Stampfl, *Langmuir* **2014**, *30*, 3787.
[7] R. Censi, W. Schuurman, J. Malda, G. di Dato, P. E. Burgisser, W. J. A. Dhert, C. F. van Nostrum, P. di Martino, T. Vermonden, W. E. Hennink, *Adv. Funct. Mater.* **2011**, *21*, 1833.
[8] S. H. Lee, J. J. Moon, J. L. West, *Biomaterials* **2008**, *29*, 2962.
[9] Y. F. Poon, Y. Cao, Y. Liu, V. Chan, M. B. Chan-Park, *ACS Appl. Mater. Interfaces* **2010**, *2*, 2012.
[10] S. Khetan, J. A. Burdick, *Biomaterials* **2010**, *31*, 8228.
[11] X. H. Qin, J. Torgersen, R. Saf, S. Muhleder, N. Pucher, S. C. Ligon, W. Holnthoner, H. Redl, A. Ovsianikov, J. Stampfl, R. Liska, *J. Polym. Sci., Part A: Polym. Chem.* **2013**, *51*, 4799.
[12] R. G. Wylie, S. Ahsan, Y. Aizawa, K. L. Maxwell, C. M. Morshead, M. S. Shoichet, *Nat. Mater.* **2011**, *10*, 799.
[13] L. Almany, D. Seliktar, *Biomaterials* **2005**, *26*, 2467.
[14] I. Frisman, Y. Shachaf, D. Seliktar, H. Bianco-Peled, *Langmuir* **2011**, *27*, 6977.
[15] Y. Shachaf, M. Gonen-Wadmany, D. Seliktar, *Biomaterials* **2010**, *31*, 2836.
[16] B. D. Fairbanks, M. P. Schwartz, C. N. Bowman, K. S. Anseth, *Biomaterials* **2009**, *30*, 6702.
[17] J. C. Crocker, D. G. Grier, *J. Colloid Interface Sci.* **1996**, *179*, 298.
[18] B. R. Dasgupta, S. Y. Tee, J. C. Crocker, B. J. Frisken, D. A. Weitz, *Phys. Rev. E* **2002**, *65*, 051505.
[19] V. Pelletier, N. Gal, P. Fournier, M. L. Kilfoil, *Phys. Rev. Lett.* **2009**, *102*, 188303.
[20] D. Ernst, J. Kohler, *Phys. Chem. Chem. Phys.* **2013**, *15*, 845.

Adv. Mater. **2015**,
DOI: 10.1002/adma.201404185